Anal Bioanal Chem
DOI 10.1007/s00216-016-0123-7

RESEARCH PAPER

A sensitive aptasensor based on molybdenum carbide nanotubes and label-free aptamer for detection of bisphenol A

Meng-Qi He[1] · Kun Wang[1] · Jin Wang[1] · Yong-Liang Yu[1] · Rong-Huan He[1]

Received: 16 September 2016 / Revised: 19 November 2016 / Accepted: 28 November 2016

Abstract To specifically and sensitively identify bisphenol A (BPA) with a simple and rapid method is very important for food safety. Using an anti-BPA aptamer and Mo_2C nanotubes, we developed a label-free and low-background signal biosensor for BPA detection. The anti-BPA aptamer drastically increased the fluorescence signal of *N*-methylmesoporphyrin IX under an assistance of Help-DNA. Additionally, BPA can interact with the anti-BPA aptamer and switch its conformation to prevent the formation of a G-quadruplex, resulting in fluorescence quenching. Simultaneously, Mo_2C nanotubes can reduce the background signals due to the adsorption of Help-DNA on their surface. This method shows a linear range of 2–20 nM with a detection limit of 2 nM for detecting BPA. This label-free BPA aptasensor with low background signal is inexpensive, easy to use, and can be applied to determine BPA in real water samples.

Keywords Biosensor · Aptamer · Label-free · Mo_2C nanotubes · Bisphenol A

Meng-Qi He and Kun Wang contributed equally to this work.

Electronic supplementary material The online version of this article (doi:10.1007/s00216-016-0123-7) contains supplementary material, which is available to authorized users.

✉ Yong-Liang Yu
yuyl@mail.neu.edu.cn

✉ Rong-Huan He
herh@mail.neu.edu.cn

[1] Department of Chemistry, College of Sciences, Northeastern University, Shenyang 110819, China

Introduction

Bisphenol A (BPA) is a key monomer in the production of polycarbonate plastic and epoxy resins [1, 2], which have been widely used in a variety of common consumer goods, e.g., water bottles, food cans, and medical devices [3, 4]. However, BPA is an endocrine-disrupting compound that can mimic the functions of estradiol and may have negative effects on human health [5–7]. Recently, the safety of BPA has been widely examined in studies on metabolic diseases, cancers, neurological effects, and environmental risk. Given its health risks, BPA was banned from use in baby bottles by the United States Food and Drug Administration in 2012 [8] and the BPA content of both carbonate resins and its derivatives should not exceed 0.05 mg kg^{-1} in China according to the Chinese Health Standard (GB 13116-91, GB 14942-94) [9]. Therefore, to prevent adverse effects on food safety and human health, it is important to detect trace amounts of BPA with high sensitivity and selectivity.

Various strategies have been reported for BPA detection, e.g., high-performance liquid chromatography (HPLC) [10], liquid chromatography (LC) [11], and gas chromatography coupled with mass spectrometry (GC-MS) [12]. The high sensitivity of these techniques has been verified, but the requirements on strict sample preparation and expensive instrumentation restrict their widespread applications [13–15]. Therefore, a sensitive and simple analytical method for quantifying BPA is urgently needed. Nanomaterials show potential applications in a variety of detection sensors because of their unique features [16, 17], e.g., electrochemical [18, 19], fluorescent [20, 21], and optical [22, 23] properties. With the increasing development of nanotechnology, the selectivity of nanomaterials has received more attention. Numerous nanomaterials have been successfully used to distinguish between single-stranded DNA (ssDNA) and double-stranded

Published online: 15 December 2016

DNA, including carbon nanotubes [24, 25], graphene oxide [26, 27], and gold nanoparticles [28, 29], and they have been used as biosensors for detection. Hence, a nanomaterial-based label-free platform is needed to develop a sensitive and specific detection method with simple, rapid, and low-background features.

Mo_2C nanotubes, as novel transition metal carbides [30], are two-dimensional (2D) ultrathin nanosheets containing more active sites than other nanomaterials. Their well-organized hierarchical hollow architecture reduces the area of overlap and aggregation [31]. Mo_2C nanotubes have been used in high-performance hydrogen evolution reactions as a highly efficient electrocatalyst [32, 33]. However, a few studies on Mo_2C nanotube bound to aptamers have been reported. It has been demonstrated that the Mo_2C nanotubes have strong selective adsorption ability to ssDNA. Xing et al. developed an efficient nanosensor for DNA detection derived from the enriched nanoporosity and large active surface of these highly dispersed nanowires with uniform Mo_2C nanocrystallites. However, dye-labeled ssDNA increased the cost and made the procedure more complex [34].

Herein, we report a novel sensing platform based on Mo_2C nanotubes and an anti-BPA aptamer for the simple, rapid, and sensitive detection of BPA. In the absence of BPA, the anti-BPA aptamer was hybridized to Help-DNA. Complexation between the anti-BPA aptamer and Help-DNA facilitated the formation of a G-quadruplex between G-rich splits GGGT of the anti-BPA aptamer and G-rich sequence (TGGGTGGG TGGGT) at the 5′-terminal of the Help-DNA [35]. The G-quadruplex structure is a guanine-rich sequence that binds to the small molecule dye *N*-methylmesoporphyrin IX (NMM). This G-quadruplex structure drastically increased the fluorescence signal of NMM [36]. In contrast, BPA can interact with the anti-BPA aptamer and switch its conformation to prevent formation of the G-quadruplex, resulting in fluorescence quenching. Simultaneously, the Mo_2C nanotubes can adsorb Help-DNA to reduce the background signals of G-rich sequences (TGGGTGGGTGGGT). We constructed a novel label-free, low-background signal sensory system for BPA detection. This label-free and low-background signal BPA aptasensor is inexpensive, easy to use, and can be applied to detect BPA in real water samples. This method shows linearity in the range of 2–20 nM with a detection limit of 2 nM for detecting BPA.

Materials and methods

Materials and reagents

Anti-BPA aptamer (5′-CCGGT GGGTG GTCAG GTGGG ATAGC GTTCC GCGTA TGGCC CAGCG CATCA CGGGT TCGCA CCA-3′), Help-DNA (5′-GAACG CTATC CACCT GACCT GGGTG GGTGG GT-3′), and FAM (5-carboxy fluorescein)-AptBPA (5′FAM-CCGGT GGGTG GTCAG GTGGG ATAGC GTTCC GCGTA TGGCC CAGCG CATCA CGGGT TCGCA CCA-3′) were synthesized by Sangon Biotechnology Co., Ltd. (Shanghai, China). Oligonucleotides were stored at −20 °C and heated to 90 °C for 10 min, followed by gradual cooling to room temperature before use to ensure that the nucleic acids were completely hybridized to each other. NMM was purchased from Porphyrin Products (Logan, UT, USA). Other chemicals were purchased from Aladdin reagent (Shanghai, China) and used as received without further purification. All reagents used were of analytical reagent grade unless specified. Milli-Q ultrapure water of 18 MΩ cm was used throughout the study.

Synthesis of Mo_2C nanotubes

The Mo_2C nanotubes were prepared as described previously [31]. First, MoO_3 nanorods were synthesized using the solvothermal method as follows: 1.4 g of ammonium heptamolybdate tetrahydrate ($(NH_4)_6Mo_7O_{24}{\cdot}4H_2O$) was dissolved in 40 mL of H_2O and 65% HNO_3 in a volume ratio of 5:1. The mixture was then transferred into a Teflon-lined stainless steel autoclave and heated at 200 °C for 12 h. After cooling, the obtained MoO_3 nanorods were washed with water and ethanol several times and then 100 mg of MoO_3 nanorods was added to 20 mL of H_2O. After ultrasonic dispersion, 200 mg of $(NH_4)_6Mo_7O_{24}{\cdot}4H_2O$ and 50 mg of dopamine hydrochloride were dissolved into the above solution, resulting in an orange-red suspension. Into the above solution, 40 mL of ethanol was added. After stirring for another 5 min, 0.3 mL of 25–28% $NH_3{\cdot}H_2O$ was quickly injected into the above reaction solution and the mixed solution reacted for 120 min with gentle stirring. Finally, the orange-red precipitate was collected by centrifugation, washed twice with ethanol, and dried under vacuum at 37 °C. The orange-red product was then annealed at 750 °C under N_2 gas flow for 16 h with a ramp rate of 5 °C min^{-1} to obtain the Mo_2C nanotubes (Mo_2C NTs).

BPA detection

The aptamer of BPA (Apt_{BPA}) and Help-DNA (H-DNA) were premixed in 25 mM Tris–HCl buffer containing 20 mM KCl and 20 mM $MgCl_2$ at pH 8.0. The premixed solution was heated at 90 °C for 10 min and gradually cooled to room temperature to form Apt_{BPA}/H-DNA. The assay solution containing 0.5 μM Apt_{BPA}/H-DNA complex, 1 μM NMM, and 60 μg mL^{-1} Mo_2C NTs in 25 mM Tris–HCl buffer was incubated for 30 min. The signal value was calculated according to the relative fluorescence intensity $(F_0 - F)/F_0$, where F_0 and F represented the fluorescence intensities of the Mo_2C NTs-based sensor system at λ_{em} 610 nm in the absence and

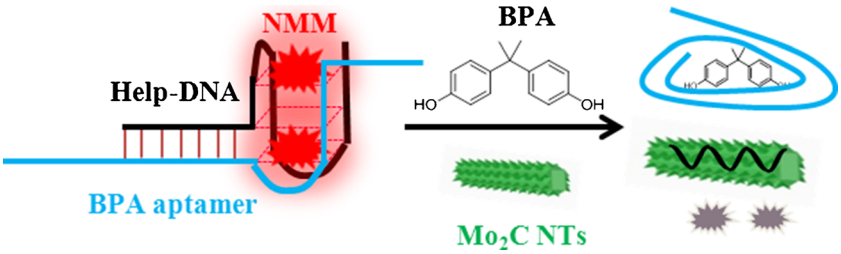

Scheme 1 Principle for label-free BPA detection

presence of BPA, respectively. For investigating the linear relationship between the concentration of BPA and $(F_0 - F)/F_0$, a series of concentrations of BPA were added to the assay solution, and the fluorescence spectra were recorded at room temperature on an F-7000 fluorescence spectrophotometer (Hitachi, Tokyo, Japan) by irradiating NMM at λ_{ex} 399 nm. Absorbance measurements were performed on a U-3900 UV–vis spectrophotometer (Hitachi). The same procedure was performed to estimate the selectivity of the present system by replacing BPA with other interferences.

Real water samples

The real water sample was collected from the Hun River (Shenyang, China). Prior to the analysis, the water samples were filtered through a 0.22-μm membrane. Next, the water samples were diluted in Tris–HCl buffer in a ratio of 1:4. The water samples, containing BPA at a specific concentration, were analyzed by following the same procedure as that used for BPA detection.

Results and discussion

Principle of the label-free fluorescent strategy for BPA detection

We found a "TGGGT" sequence in the anti-BPA aptamer. Hence, H-DNA, with a G-rich sequence (TGGGTGGG TGGGT) at the 5′ terminus, was utilized to form the G-quadruplex structure with the anti-BPA aptamer. A weaker signal was observed for NMM alone (see Electronic Supplementary Material (ESM) Fig. S1A(a)), but the formed G-quadruplex structure drastically increased the fluorescence signal of NMM (ESM Fig. S1A(b)). The anti-BPA aptamer shows high binding affinity to BPA ($K_d = 8.3$ nM), as described by Jo et al. [37]. In the presence of BPA, structural changes were induced in the aptamers, preventing the formation of the G-quadruplex, resulting in dissociative quenching (ESM Fig. S1A(c)). However, the H-DNA still generated a high background signal because of the fluorescence intensity from the short G-rich strands G3. In order to reduce the

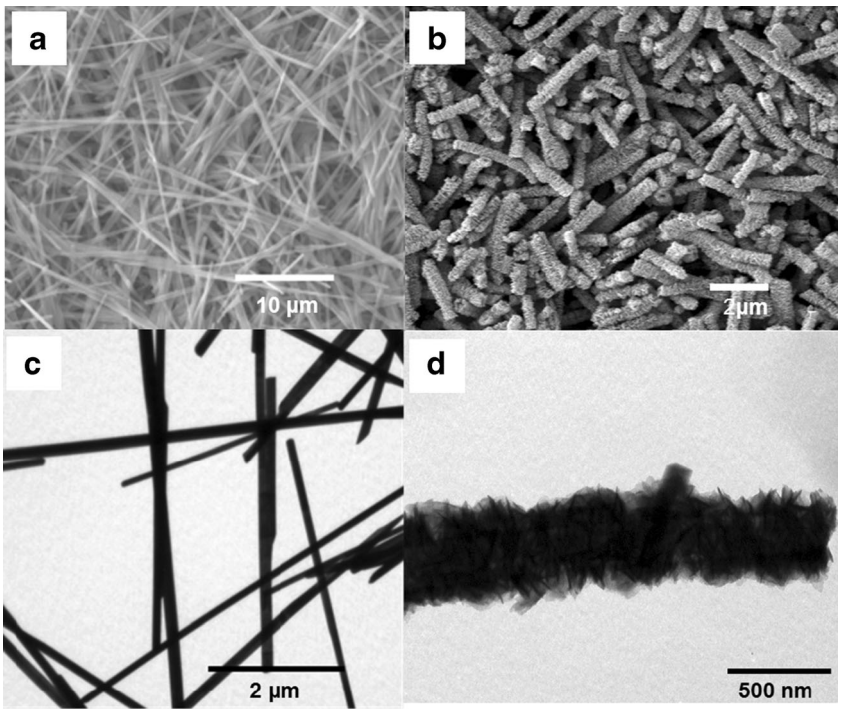

Fig. 1 SEM and TEM characterization of prepared MoO_3 NRs (**a** and **c**) and Mo_2C NTs (**b** and **d**), respectively

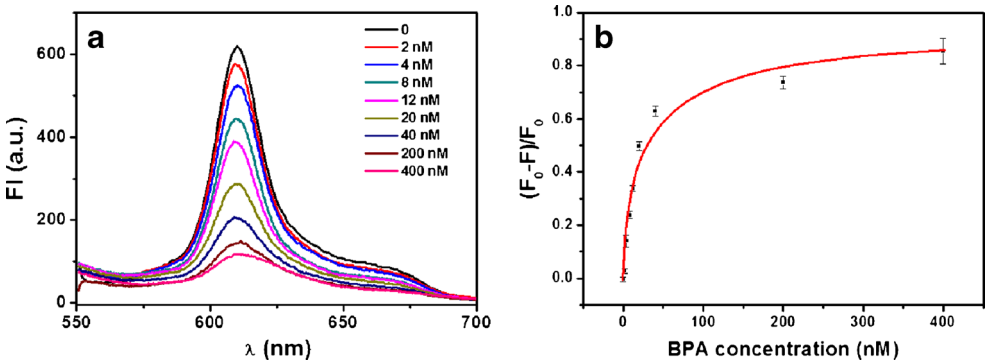

Fig. 2 **a** Fluorescence spectra of NMM as a function of different concentrations of BPA. **b** Peak fluorescence change ($(F_0 - F)/F_0$) as a function of BPA concentration

influence of H-DNA, Mo_2C nanotubes were used to adsorb dissociative H-DNA. Nevertheless, BPA aptamer as a single-strand DNA may also be adsorbed on the Mo_2C NTs. Therefore, the binding kinetics between Apt_{BPA} and Mo_2C NTs were investigated by modifying the FAM at the 5′ terminus of the Apt_{BPA} (FAM-Apt_{BPA}). The validation test and kinetic results prove that Apt_{BPA} can be released from Mo_2C NTs when BPA binds Apt_{BPA} to form BPA/Apt_{BPA} complex, as shown in ESM, Fig. S2 and Fig. S3. Finally, a label-free, simple, low-background BPA aptasensor was constructed (Scheme 1).

Characterization of prepared Mo_2C nanotubes

Mo_2C nanotubes play a critical role in reducing the influence of H-DNA. Thus, the properties of Mo_2C nanotubes were investigated in the following experiments. The MoO_3 nanorods were used as a reactive self-degraded template as well as additional Mo supply. These MoO_3 nanorods have a smooth surface with an average width of approximately 350 nm according to the results of scanning electron microscopy (SEM) and transmission electron microscopy (TEM) (Fig. 1a/c). The MoO_3 nanorods were employed as self-degradable templates to obtain Mo-polydopamine nanotubes. After annealing the Mo-polydopamine nanotubes, the obtained Mo_2C nanotubes showed good crystallinity based on the x-ray diffraction results (ESM Fig. S4). SEM images indicated that the prepared Mo_2C nanotubes had a rough surface and hollow interior (Fig. 1b). A TEM showed that the walls of the nanotube were constructed by 2D thin nanosheets (Fig. 1d). In this study, the MoO_3 nanorods and Mo_2C nanotubes were employed to adsorb H-DNA. The H-DNA, which was adsorbed onto the Mo_2C nanotubes, did not enhance the fluorescence of NMM. When only H-DNA was present, the system generated a background signal (ESM Fig. S1B(a)). The MoO_3 nanorods and Mo_2C nanotubes adsorbed H-DNA to decrease the background signal (ESM Fig. S1B(b/c)). However, the Mo_2C nanotubes showed superior performance to other systems, which may be attributed to the nanosheets on the Mo_2C nanotubes (Fig. 1d). The nanosheets increased the surface area of the Mo_2C nanotubes and thus increased the adsorption capacity.

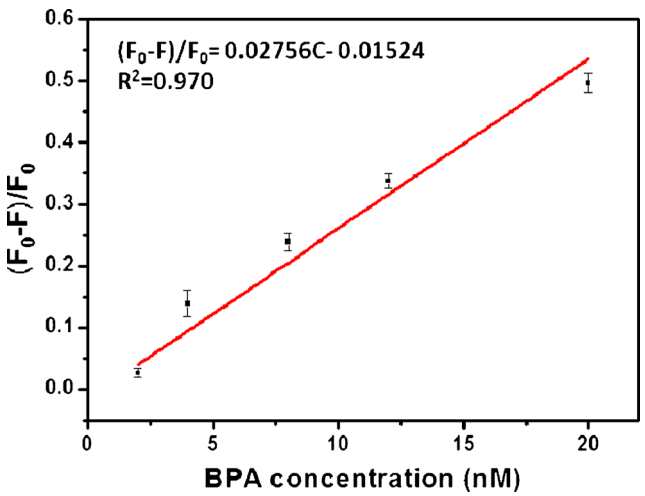

Fig. 3 Plot of the linear relationship between the peak fluorescence change ($(F_0 - F)/F_0$) and the concentration of target BPA from 2 to 20 nM

Optimization of experimental conditions for aptasensor

In addition to the influence of the Mo_2C nanotube surface, the performance of the present aptasensor is affected by the concentration of Mo_2C nanotubes which directly affects the background. The effect of Mo_2C nanotubes was investigated by monitoring the fluorescence at different concentrations of Mo_2C nanotubes. A blank sample without Mo_2C nanotubes was tested under the same conditions. Larger amounts of H-DNA were adsorbed with increasing concentrations of Mo_2C nanotubes, which decreased the background signal. Fluorescence intensity gradually decreased with increasing the concentration of Mo_2C nanotubes up to 60 μg mL^{-1} and then plateaued (ESM Fig. S5). In order to obtain the optimum detection performance, a concentration of 60 μg mL^{-1} Mo_2C nanotubes was adopted in the following experiments.

Fluorescence intensity changes also depend on the incubation time of BPA in the detection system. The optimal incubation time of BPA in the detection system was explored by

Table 1 Comparisons of the present aptasensor with those having labeled groups for BPA detection

Method	Labeled group	Detection range (nM)	LOD (nM)
Electrochemical aptasensor [9]	SH-$(CH_2)_6$	10–10,000	5[a]
Surface-enhanced Raman scattering [38]	Cy5	3–300	3[a]
Optic fiber aptasensor [39]	Cy5	2–100	1.86[a]
Label-free fluorescent aptasensor (this work)	–	2–400	0.9[a]/2[b]

[a] LOD was calculated based on the 3σ/slope

[b] LOD was determined experimentally

monitoring the fluorescence spectra change in NMM with the incubation time of BPA. The fluorescence intensity of NMM at λ_{em} 610 nm significantly decreased with increasing incubation time up to 30 min and then reached a plateau (ESM Fig. S6). Thus, 30 min was selected as the optimal incubation time.

Performance of the aptasensor

To evaluate the sensitivity and dynamic range of the proposed detection system, the fluorescence intensity change of NMM in the presence of different concentrations of BPA was monitored. In the absence of BPA, Apt_{BPA} hybridized to the H-DNA and formed the G-quadruplex to generate a high fluorescence signal. In the presence of BPA, the conformation of the G-quadruplex was destroyed with increasing BPA concentrations, decreasing the fluorescence signal. As shown in Fig. 2, a decrease in fluorescence intensity was observed with increasing BPA concentrations in the range of 0–400 nM. The fluorescence intensity of NMM at λ_{em} 610 nm linearly depended on the BPA concentration ranging from 2 to 20 nM. Figure 3 shows the corresponding calibration plot for different concentrations of BPA. Error bars with a correlation coefficient of 0.970 were obtained from three independent experiments, indicating the high reproducibility of the developed sensing system. As shown in ESM Fig. S7, the limit of detection (LOD) of 2 nM was obtained based on the experimental determination, where an obvious signal response of 2 nM BPA was observed with respect to that of blank. This detection limit meets the requirements of the Chinese Health Standard [9]. Furthermore, this aptasensor has similar analytical performances to those with labeled group, as listed in Table 1 [9, 38, 39].

Selectivity is a crucial parameter for evaluating the performance of the aptasensor. To assess the specificity of the fabricated aptasensor, we evaluated molecules with similar structures to BPA, which might interfere with the performance of the aptasensor for BPA detection, e.g., 4,4′-biphenol, bisphenol AF, and 4,4′-sulfonyldiphenol. Figure 4 shows the fluorescence spectra upon exposure of the aptasensor to these molecules and the fluorescence intensity drastically decreased in the presence of BPA. The interfering molecules only slightly decreased the background signal. The result shows that the aptasensor exhibits good selectivity for BPA. Additionally, the fluorescence decrement ratio $(F_0 - F)/F_0$ was determined to

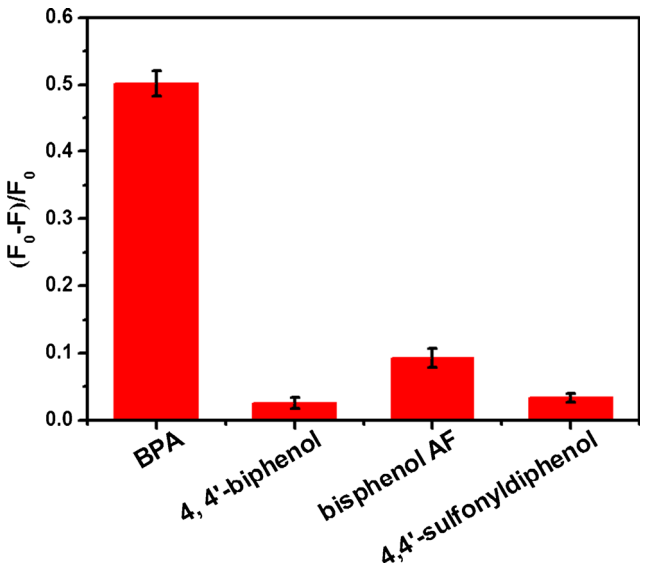

Fig. 4 Selectivity investigation of the proposed strategy for BPA detection

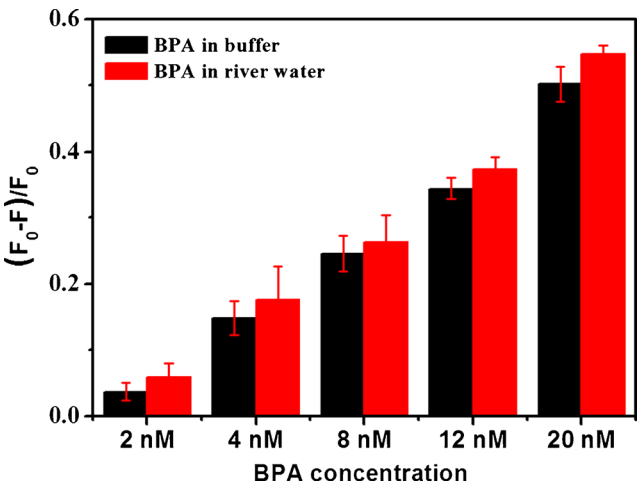

Fig. 5 Results obtained from the buffer solution and diluted real water samples spiked with different concentrations of BPA

quantify the changes when the sensor was exposed to different molecules. The results clearly indicated that the aptasensor displayed high specificity and selectivity towards BPA and thus has great potential for practical applications. This excellent selectivity can be ascribed to the specific and high affinity of anti-BPA aptamer to BPA.

Analysis of real water samples

To confirm the feasibility and sensitivity of the aptasensor for analyzing real water samples, river water (Hun River in Shenyang, China) was chosen for the evaluation of BPA detection. The same procedure as that used for the measurement of buffer solution was applied. A series of BPA solutions was prepared by spiking different amounts of BPA into 5-fold diluted actual water samples. As shown in Fig. 5, a trend similar to that observed for pure buffer solution was observed, confirming that our proposed method can be used for real water sample detection. These results confirmed the practical value of the developed biosensor.

Conclusions

We developed a convenient fluorescence assay for highly sensitive and specific detection of BPA with acceptable reproducibility. The "TGGGT" sequence in Apt_{BPA} was utilized to form a G-quadruplex structure with H-DNA (with the G-rich sequence (TGGGTGGGTGGGT) at the 5′ terminus). BPA acts as a trigger to alter the G-quadruplex structure. The superior adsorption ability of Mo_2C nanotubes reduced the background signal and enabled sensitive detection of 2 nM BPA in a buffer solution. Importantly, the developed assay can be used to distinguish BPA from other molecules with structures similar to that of BPA. This is the first report demonstrating the application of an aptasensor for BPA detection in real water samples based on label-free ssDNA and Mo_2C nanotubes. Compared with conventional methods, the developed detection strategy provides a sensitive, specific, simple, enzyme-free, and cost-effective assay and has potential practical applications.

Acknowledgements This work was financially supported by the Natural Science Foundation of China (51572044, 21475018), the Program of New Century Excellent Talents in University (NCET-13-0114), and the Fundamental Research Funds for the Central Universities (N140506001, N140505005).

Compliance with ethical standards

Conflict of interest The authors declare that they have no competing interests.

Research involving human participants and/or animals This work does not contain any studied with human participants or animals.

References

1. Vandenberg LN, Maffini MV, Sonnenschein C, Rubin BS, Soto AM. Bisphenol-A and the great divide: a review of controversies in the field of endocrine disruption. Endocr Rev. 2009;30:75–95.
2. Cui H, Wu J, Eda S, Chen J, Chen W, Zheng L. Rapid capacitive detection of femtomolar levels of bisphenol A using an aptamer-modified disposable microelectrode array. Microchim Acta. 2015;182:2361–7.
3. Xue F, Wu J, Chu H, Mei Z, Ye Y, Liu J, et al. Electrochemical aptasensor for the determination of bisphenol A in drinking water. Microchim Acta. 2013;180:109–15.
4. Lee JS, Kim SG, Jun J, Shin DH, Jang J. Aptamer-functionalized multidimensional conducting-polymer nanoparticles for an ultrasensitive and selective field-effect-transistor endocrine-disruptor sensors. Adv Funct Mater. 2014;24:6145–53.
5. Rochester JR. Bisphenol A, and human health: a review of the literature. Reprod Toxicol. 2013;42:132–55.
6. Chung E, Jeon J, Yu J, Lee C, Choo J. Surface-enhanced Raman scattering aptasensor for ultrasensitive trace analysis of bisphenol A. Biosens Bioelectron. 2015;64:560–5.
7. Xu J, Li Y, Bie J, Jiang W, Guo J, Luo Y, et al. Colorimetric method for determination of bisphenol A based on aptamer-mediated aggregation of positively charged gold nanoparticles. Microchim Acta. 2015;182:2131–8.
8. Hunt PA, Lawson C, Gieske M, Murdoch B, Smith H, Marre A, et al. Bisphenol A alters early oogenesis and follicle formation in the fetal ovary of the rhesus monkey. Proc Natl Acad Sci U S A. 2012;109:17525–30.
9. Zhou L, Wang J, Li D, Li Y. An electrochemical aptasensor based on gold nanoparticles dotted graphene modified glassy carbon electrode for label-free detection of bisphenol A in milk samples. Food Chem. 2014;162:34–40.
10. Yoon Y, Westerhoff P, Snyder SA, Esparza M. HPLC-fluorescence detection and adsorption of bisphenol A, 17 beta-estradiol, and 17 alpha-ethynyl estradiol on powdered activated carbon. Water Res. 2003;37:3530–7.
11. Zafra-Gómez A, Ballesteros O, Navalón A, Vílchez JL. Determination of some endocrine disrupter chemicals in urban wastewater samples using liquid chromatography-mass spectrometry. Microchem J. 2008;88:87–94.
12. Kawaguchi M, Inoue K, Yoshimura M, Ito R, Sakui N, Okanouchi N, et al. Determination of bisphenol A in river water and body fluid samples by stir bar sorptive extraction with in situ derivatization and thermal desorption-gas chromatography–mass spectrometry. J Chromatogr B. 2004;805:41–8.
13. Zhao M-P, Li Y-Z, Guo Z-Q, Zhang X-X, Chang W-B. A new competitive enzyme-linked immunosorbent assay (ELISA) for determination of estrogenic bisphenols. Talanta. 2002;57:1205–10.
14. Watabe Y, Kondo T, Morita M, Tanaka N, Haginaka J, Hosoya K. Determination of bisphenol A in environmental water at ultra-low level by high-performance liquid chromatography with an effective on-line pretreatment device. J Chromatogr A. 2004;1032:45–9.
15. Vandenberg LN, Chahoud I, Heindel JJ, Padmanabhan V, Paumgartten FJR, Schoenfelder G. Urinary, circulating, and tissue biomonitoring studies indicate widespread exposure to bisphenol A. Cienc Saude Coletiva. 2012;17:407–34.
16. Chen J, Duncan B, Wang Z, Wang LS, Rotello VM, Nugen SR. Bacteriophage-based nanoprobes for rapid bacteria separation. Nanoscale. 2015;7:16230–6.

17. Chen J, Li Y, Huang K, Wang P, He L, Carter KR, et al. Nanoimprinted patterned pillar substrates for surface-enhanced Raman scattering applications. ACS Appl Mater Interfaces. 2015;7:22106–13.
18. Zhang Y, Cao T, Huang X, Liu M, Shi H, Zhao G. A visible-light driven photoelectrochemical aptasensor for endocrine disrupting chemicals bisphenol A with high sensitivity and specificity. Electroanalysis. 2013;25:1787–95.
19. Yu P, Liu Y, Zhang X, Zhou J, Xiong E, Li X, et al. A novel electrochemical aptasensor for bisphenol A assay based on triple-signaling strategy. Biosens Bioelectron. 2016;79:22–8.
20. Long F, Zhu A, Shi H, Wang H. Hapten-grafted graphene as a transducer for homogeneous competitive immunoassay of small molecules. Anal Chem. 2014;86:2862–6.
21. Duan N, Zhang H, Nie Y, Wu S, Miao T, Chen J, et al. Fluorescence resonance energy transfer-based aptamer biosensors for bisphenol A using lanthanide-doped $KGdF_4$ nanoparticles. Anal Methods. 2015;7:5186–92.
22. Wang K, Fan D, Liu Y, Wang E. Highly sensitive and specific colorimetric detection of cancer cells via dual-aptamer target binding strategy. Biosens Bioelectron. 2015;73:1–6.
23. Zhang D, Yang J, Ye J, Xu L, Xu H, Zhan S, et al. Colorimetric detection of bisphenol A based on unmodified aptamer and cationic polymer aggregated gold nanoparticles. Anal Biochem. 2016;499:51–6.
24. Zhang Y, Li B, Yan C, Fu L. One-pot fluorescence detection of multiple analytes in homogenous solution based on noncovalent assembly of single-walled carbon nanotubes and aptamers. Biosens Bioelectron. 2011;26:3505–10.
25. Deng W, Shen L, Wang X, Yang C, Yu J, Yan M, et al. Using carbon nanotubes-gold nanocomposites to quench energy from pinnate titanium dioxide nanorods array for signal-on photoelectrochemical aptasensing. Biosens Bioelectron. 2016;82:132–9.
26. Wang K, Ren J, Fan D, Liu Y, Wang E. Integration of graphene oxide and DNA as a universal platform for multiple arithmetic logic units. Chem Commun. 2014;50:14390–3.
27. Zhu Y, Cai Y, Xu L, Zheng L, Wang L, Qi B, et al. Building an aptamer/graphene oxide FRET biosensor for one-step detection of bisphenol A. ACS Appl Mater Interfaces. 2015;7:7492–6.
28. Liu JM, Yan XP. Competitive aptamer bioassay for selective detection of adenosine triphosphate based on metal-paired molecular conformational switch and fluorescent gold nanoclusters. Biosens Bioelectron. 2012;36:135–41.
29. Kuang H, Yin H, Liu L, Xu L, Ma W, Xu C. Asymmetric plasmonic aptasensor for sensitive detection of bisphenol A. ACS Appl Mater Interfaces. 2014;6:364–9.
30. Chen WF, Wang CH, Sasaki K, Marinkovic N, Xu W, Muckerman JT, et al. Highly active and durable nanostructured molybdenum carbide electrocatalysts for hydrogen production. Energy Environ Sci. 2013;6:943–51.
31. Ma FX, Wu HB, Xia BY, Xu CY, Lou XW. Hierarchical beta-Mo_2C nanotubes organized by ultrathin nanosheets as a highly efficient electrocatalyst for hydrogen production. Angew Chem Int Ed. 2015;54:15395–9.
32. Xiao P, Ge X, Wang H, Liu Z, Fisher A, Wang X. Novel molybdenum carbide-tungsten carbide composite nanowires and their electrochemical activation for efficient and stable hydrogen evolution. Adv Funct Mater. 2015;25:1520–6.
33. Vrubel H, Hu X. Molybdenum boride and carbide catalyze hydrogen evolution in both acidic and basic solutions. Angew Chem Int Ed. 2012;51:12703–6.
34. Xing Z, Wang L, Sun X, He Y, Asiri AM. Nanoporous molybdenum carbide nanowires: a novel sensing platform for DNA detection. J Mater Chem B. 2015;3:7173–6.
35. Siddiqui-Jain A, Grand CL, Bearss DJ, Hurley LH. Direct evidence for a G-quadruplex in a promoter region and its targeting with a small molecule to repress c-MYC transcription. Proc Natl Acad Sci U S A. 2002;99:11593–8.
36. Oh SS, Plakos K, Lou XH, Xiao Y, Soh HT. In vitro selection of structure-switching. Self-reporting aptamers. Proc Natl Acad Sci U S A. 2010;107:14053–8.
37. Jo M, Ahn JY, Lee J, Lee S, Hong SW, Yoo JW, et al. Development of single-stranded DNA aptamers for specific bisphenol A detection. Oligonucleotides. 2011;21:85–91.
38. Marks HL, Pishko MV, Jackson GW, Cote GL. Rational design of a bisphenol A aptamer selective surface-enhanced Raman scattering nanoprobe. Anal Chem. 2014;86:11614–9.
39. Yildirim N, Long F, He M, Shi HC, Gu AZ. A portable optic fiber aptasensor for sensitive, specific and rapid detection of bisphenol-A in water samples. Environ Sci Process Impacts. 2014;16:1379–86.